JOURNAL DE PHYSIQUE IV
Colloque C5, supplément au Journal de Physique II, Volume 5, juin 1995

Low Pressure CVD of Silicon Nitride from a Silane-Ammonia Mixture: Analysis of Preliminary Experimental and Simulation Results

K. Yacoubi, C. Azzaro and J.P. Couderc

ENSIGC INPT, Laboratoire de Génie Chimique, URA 192 du CNRS, 18 Chemin de la Loge, 31078 Toulouse cedex, France

Abstract : Results of a study dealing with the deposition of silicon nitride from a silane-ammonia mixture and combining experimental approach and deposition modelling are presented. First, a thorough QRKK analysis has compensated for the lack of kinetic information in the gas phase. A reduced reaction set reproducing the essential features of the full mechanism and involving 6 species including two silylamine intermediates SiH_3NH_2 and $SiHNH_2$ has been identified. A local two-dimensional model previously developed in our laboratory has then been adapted to the treatment of silicon nitride deposition. The identification of the kinetic parameters of the heterogeneous mechanism has been achieved through a combined approach of experimental and simulation results.

1. INTRODUCTION

LPCVD has become a classical production method for silicon nitride films, commonly used as insulation or passivation materials within the MOS technology. When this kind of deposition is carried out from a silane-ammonia mixture, the following processing difficulties may be encountered:
(i)-Growth rate decreases markedly relative to pure polysilicon deposition;
(ii)-A significant radial nonuniformity is reported, both in deposition rate and film composition;
(iii)-A longitudinal decrease in deposition rate is generally observed.

In spite of its importance and difficulties, the case of silicon nitride has surprisingly received little attention. Only the deposition from a mixture of dichlorosilane and ammonia, presenting the same general trends as those reported from a silane-ammonia source, has been treated in the literature [1]. Results of this study indicate that the in-wafer film thickness nonuniformities may be explained by the effect of diffusion-limited film growth from highly reactive gas-phase intermediates, with simultaneous deposition from less reactive dichlorosilane.

The purpose of this work is to combine both modelling and experimental analysis in order to elucidate the complex physicochemical phenomena involved in the deposition process from a silane-ammonia mixture.

Due to the lack of kinetic information available in the literature, a major part of this work has been focused on the investigation of gas phase reactions. In the first part of this paper, the results of a thorough QRRK (Quantum Rice Ramsberger Kassel) analysis compensating for the lack of kinetic information will be presented. Then, first experimental results of silicon nitride deposition will be presented and analysed. They will be compared with the predictions of the CVD2 model previously developed in our laboratory [2]. The extension principles of the CVD2 model to the case of silicon nitride will be discussed. It must be pointed out that the results presented in this paper are preliminary, but that a promising agreement between experimental and simulation results has been obtained. Perspectives of this work will finally be suggested.

2. THERMAL DECOMPOSITION OF A SILANE-AMMONIA MIXTURE

To our knowledge, the kinetics of thermal decomposition of a mixture of silane and ammonia has received very little attention in the literature. In this study, the following reactions have been taken into account [4]:

Type of reactions [References]	Chemical mechanism	/ Remarks
Silane pyrolysis [3]	$SiH_4 \rightleftharpoons SiH_2 + H_2$ $SiH_4 \rightleftharpoons SiH_3 + H$ $Si_2H_6 \rightleftharpoons SiH_4 + SiH_2$	- Extensively studied -The formation of higher order silanes is negligible [3]
Ammonia pyrolysis [5]	$NH_3 \rightleftharpoons NH_2 + H$	
Ammonia-silicon hydrides reactions [4]	$SiH_4 + NH_3 \rightleftharpoons SiH_3NH_2 + H_2$	$SiH_2 + NH_3 \rightleftharpoons SiH_3NH_2$
Pyrolysis of SiH_3NH_2 [4]	$SiH_3NH_2 \rightleftharpoons SiHNH_2 + H_2$ $SiH_3NH_2 \rightleftharpoons SiH_2NH + H_2$	$SiH_3NH_2 \rightleftharpoons SiH_2NH_2 + H$ $SiH_3NH_2 \rightleftharpoons SiH_3 + NH_2$
Molecule-radical and radical-radical reactions [6]	$NH_3 + H \rightleftharpoons NH_2 + H_2$ $NH_2 + NH_2 \rightleftharpoons N_2H_4$ $NH_3 + NH_2 \rightleftharpoons N_2H_4 + H$ $NH_2 + SiH_4 \rightleftharpoons SiH_3NH_2 + H$ $NH_3 + SiH_3 \rightleftharpoons SiH_3NH_2 + H$	$NH_2 + SiH_4 \rightleftharpoons SiH_3 + NH_3$ $SiH_4 + H \rightleftharpoons SiH_3 + H_2$ $SiH_4 + SiH_3 \rightleftharpoons Si_2H_6 + H$ $SiHNH_2 + H \rightleftharpoons SiH_2NH_2$ $SiH_2NH + H \rightleftharpoons SiH_2NH_2$

Table 1 : Homogeneous gas phase reactions

Different methods have been used to evaluate unknown rate constants (carbon hydrides analogies, collision frequency limits, Benson's method [7]) at P=1 atm and T = 298°K. Using these evaluations, or measured constants in other conditions (note that they are only available for silane pyrolysis), rate constants of unimolecular or bimolecular reactions deduced from the reactions presented in Table 1, corresponding to LPCVD conditions, i.e. to the pressure fall-off region, have been calculated with QRRK theory [8]. Note that this theory has been successful in predicting the reduction of the unimolecular rate constants with decreasing pressure for silane or SIPOS decomposition [8] and the estimation of bimolecular rate constants. A detailed presentation of the QRRK model used can be found in [8]. By lack of place, kinetic rate constants of the whole mechanism will not be presented.

Using that mechanism, the time evolution of all the species concentrations which could be observed in a hypothetical gas volume, uniform in its properties and without any contact with solid surfaces, starting from the mixture of silane and ammonia has been computed using numerical integration based on Gear's method [9]. Typical results obtained are presented in Figure 1 for a temperature of 750°C, a pressure set at 0.4 Torr and a silane/ammonia ratio equal to 0.4/0.6

A distinction must be made between radical and stable species :

On the one hand, disilane and hydrazine, which are stable molecules, have very low concentrations relative to the concentrations of the other stable species, i. e. silane and hydrogen. A series of simulation runs was performed in which secondary reactions of these species were neglegted. The results obtained showed that the evolution of the remaining species of the system is not affected by this modification.

On the other hand, even in very low concentrations, silylamine radicals ($SiHNH_2$, SiH_2NH and SiH_2NH_2) may have a non negligible impact on the whole mechanism. Due to the similar atomic structure of these species, it could be assumed that their contribution to deposition rate was directly dependent on the molar fraction of the species. As $SiHNH_2$ molar fraction is approximately 10^4 times greater than the other ones, its contribution will mask the effect of the other species.

A similar analysis has been applied to the cases of SiH_2 and SiH_3. It has led to the elimination of SiH_3 in the chemical mechanism (see Figure 2). This approach has been repeated for a wide range of temperatures, pressures and silane/ammonia ratios. In all cases, the same species have been candidates for elimination and have been finally removed from the complete scheme.

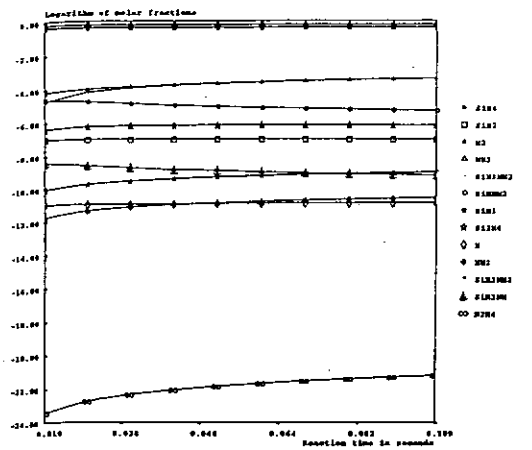

Figure 1 : Time evolution of the species concentrations (Complete mechanism)

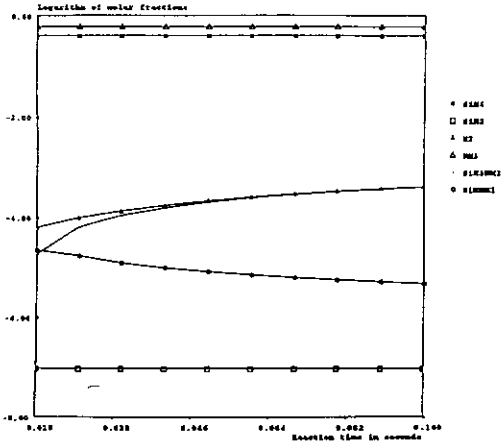

Figure 2 : Time evolution of the species concentrations (Reduced mechanism)

Finally, a reduced reaction set (see Table 2) which reproduces the essential features of the full mechanism and involves only 6 species including two silylamine intermediates, i.e., SiH_3NH_2 (stable) and $SiHNH_2$ (reactive) has been adopted.

Chemical reaction	Kinetic constants (results of QRRK analysis) ($R = 8.314$ J mole^{-1} K^{-1}, P in [Pa])
$SiH_2 + H_2 \rightleftharpoons SiH_4$	$k_1 = 0{,}074\ P \exp(66.27\ 10^3/RT)$ [m^3 mole^{-1} s^{-1}] $k_{-1} = 1{,}3810^8\ P \exp(-209.65\ 10^3/RT)$ [s^{-1}]
$SiH_2 + NH_3 \rightleftharpoons SiH_3NH_2$	$k_2 = 4{,}082\ 10^4 \exp(34.97\ 10^3/RT)$ [m^3 mole^{-1} s^{-1}] $k_{-2} = 9{,}21\ 10^4 \exp(16.18\ 10^3/RT)$ [s^{-1}]
$SiH_2 + NH_3 \rightleftharpoons SiHNH_2 + H_2$	$k_3 = 17{,}4\ 10^{-3}\ P \exp(64.53\ 10^3/RT)$ [m^3 mole^{-1} s^{-1}] $k_{-3} = 3{,}23\ 10^8\ P \exp(-217.51\ 10^3/RT)$ [m^3 mole^{-1} s^{-1}]
$SiHNH_2 + H_2 \rightleftharpoons SiH_3NH_2$	$k_4 = 1{,}781\ 10^{-2}\ P^{0,87} \exp(121.4\ 10^3/RT)$ [m^3 mole^{-1}s^{-1}] $k_{-4} = 9{,}68\ 10^8\ P^{0,97} \exp(-178.09\ 10^3/RT)$ [s^{-1}]

Table 2 : Homogeneous gas phase mechanism adopted in this study

3. EXPERIMENTAL STUDY

3. 1 Operating conditions

Experiments were carried out in a conventional tubular horizintal hot-wall LPCVD reactor, in which 82 p-type <100> Si wafers were stacked vertically inside the reactor. The main characteristics of the equipment used are presented in Table 3. Four test wafers were placed at selected locations along the length of reactor (57, 62, 67, 72 th). The position of each wafer in the batch is numbered from the first wafer reached by the gases. Three boats were used and placed coaxially in the reactor one after another. The boats are separated by a distance of 5 cm. The first boat is placed next to the inlet door of the reactor and the test wafers are placed inside the flat temperature zone of the reactor. Experiments were

performed at two temperatures 650°C and 750°C. Pressure was set at 0.4 Torr. As gaseous sources, pure silane and ammonia with a ratio 0.4/0.6 were used. Silane flowrate was maintained at 180 sccm and 270 sccm of ammonia was injected. Film thickness was measured by ellipsometry at a wavelength of 405 nm. The results obtained were confirmed by plasma etching and measurements of the height of the chemically created step with TENCOR equipment.

Geometrical parameters	
Tube length [m]	1.97
Tube diameter [mm]	135
Wafer diameter [mm]	100.4
Interwafer distance [mm]	8
Boat number	3
Wafer number in each boat	28/28/26

Table 3 : Reactor geometry

3. 2 Experimental results

The longitudinal evolution of silicon nitride deposition rate measured in the center of each wafer is shown in Figure 3. It can be first seen that the presence of ammonia reduces markedly deposition rate (relative to pure polysilicon deposition). To give an order of comparison, pure polysilicon deposition rate is about 100 Å/min at 600°C. Second, it can be seen that, at both temperatures, the deposition rate is higher on the first test wafers and then tends to a quasi uniform deposition rate on the last test wafers.

Figure 4 relative to 4th test wafer of the load shows typical radial deposition rate profiles. Significant non-uniformities appear at the wafer periphery, creating the so-called "bull's eye effect". These results will be analysed in the following sections.

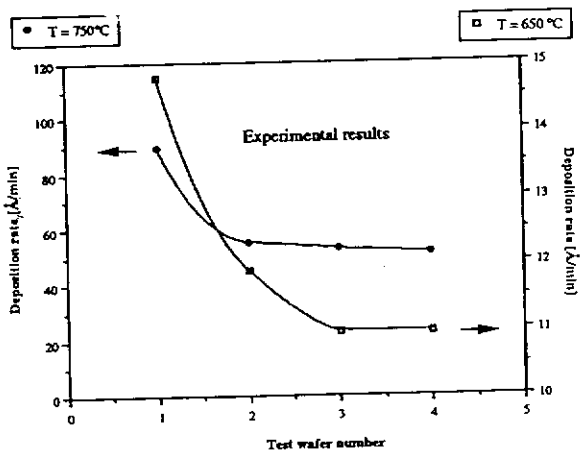

Figure 3 : Longitudinal evolution of silicon nitride deposition rate

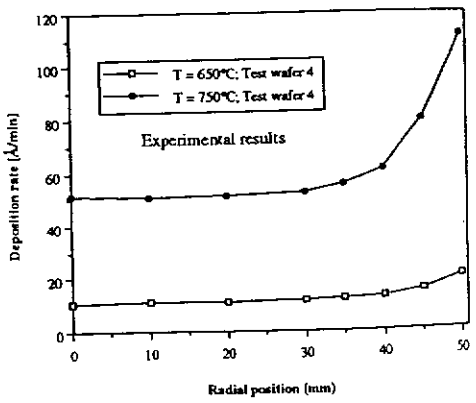

Figure 4 : Radial silicon nitride deposition rate

4. MODELLING OF SILICON NITRIDE DEPOSITION

4. 1 Basic principles

A local two-dimensional model called CVD2 was developed previously in our laboratory [2] and led to very satisfying results concerning in situ phosphorus doped polysilicon deposition or SIPOS deposition

[2, 9]. Note that these depositions show a remarkable similarity to data for the deposition of silicon nitride. Let us recall that CVD2 is limited to a small but representative part of the reactor, i.e. an interwafer spacing and the corresponding annular region between the wafer edge and the reactor walls. In this modelling field, the continuity and Navier-Stokes equations on the one hand and the mass balance equations for every chemical species on the other hand are solved, respectively, for gas flow and mass transport. A detailed presentation of the modelling principles of CVD2 is provided in [2]. In this paper, only the new elements introduced to extend the model to the case of silicon nitride deposition will be developed.

The creation and consumption of the chemical species due to the homogeneous gas phase reactions previously determined are taken into account in the mass balance equations.

All the chemical species containing silicon and/or nitrogen can react on solid surfaces to deposit silicon nitride. Table 4 shows the surface reactions that we consider for this system.

Surface reactions	Deposition rate expression [mol m^{-2} s^{-1}]	Kinetic constants
$SiH_4 \rightarrow Si + 2\,H_2$	$\dfrac{k_1 P_{SiH_4}}{1 + k_S P_{SiH_4} + k_H P_{SiH_4} + k_N P_{NH_3}}$	$k_1 = 0.973\ 10^{-7}$ [mol m^{-2} s^{-1}Pa^{-1}] $k_S = 0.83\ 10^{-10} \exp(18000/T)$ [mol m^{-2} s^{-1}] $k_H = 4.8\ 10^{-8} \exp(10000/T)$ [mol m^{-2} s^{-1}] $k_N = 0.88\ 10^{-10} \exp(20000/T)$ [mol m^{-2} s^{-1}] $k_2 = 0.1775\ 10^{-6}$ [mol m^{-2} s^{-1}Pa^{-1}]
$NH_3 \rightarrow N + 3/2\,H_2$	$\dfrac{k_2 P_{NH_3}}{1 + k_S P_{SiH_4} + k_H P_{SiH_4} + k_N P_{NH_3}}$	
$SiH_2 \rightarrow Si + H_2$	$\gamma_{SiH_2} \sqrt{\dfrac{RT}{2\,\Pi\,M_{SiH_2}}} \dfrac{P_{SiH_2}}{RT}$	$\gamma_{SiH2} = 1$ $\quad \Pi = 3.1416$ $M_{SiH2} = 30$ g
$SiHNH_2 \rightarrow Si + N + 3/2\,H_2$	$\gamma_{SiHNH_2} \sqrt{\dfrac{RT}{2\,\Pi\,M_{SiHNH_2}}} \dfrac{P_{SiHNH_2}}{RT}$	$\gamma_{SiHNH2} = 1$ $\quad \Pi = 3.1416$ $M_{SiHNH2} = 45$ g

Table 4 : Kinetic expressions for surface reactions

A Langmuir-Hinshelwood approach has been used to represent the respective contributions of silane and ammonia to silicon nitride deposition. The kinetic constants k_H and k_S given by Wilke et al. [10] were adopted. The kinetic adsorption constant k_N was introduced to reflect the reduction of silane contribution in presence of ammonia, as suggested by experimental results. A similar form of the rate equation was adopted for ammonia deposition. The kinetic constants k_1, k_2 and k_N at 750°C were adjusted after trial and error tests based on comparison between experimental and simulation results.

As in our earlier modelling work concerning in situ phosphorus doped polysilcon deposition, we assume that any reactive intermediate (SiH_2 or $SiHNH_2$) that strikes the surface reacts with unit probability. The reaction rates of SiH_2 and of $SiHNH_2$ are first-order dependent on their respective concentrations. In these expressions, γ_i represents the sticking coefficient of species i. This coefficient has been taken equal to unity, as suggested by other investigators [4] for silylene. Due to the reactive nature of $SiHNH_2$, a same value has been adopted for this species.

As first approach, due to its saturated nature, the deposition of silicon nitride from saturated molecule SiH_3NH_2 has been assumed to be negligible. A similar hypothesis was adopted for disilane Si_2H_6 in the case of silicon deposition [2, 9, 11].

The choice of the boundary conditions at the entrance and the exit is complicated by the limitation of the modelling field to a representative interwafer space. In previous studies [2, 8], the basic assumption to overcome this difficulty is that, far from the ends of the wafer line, a large number of phenomena linked to flow and mass transport processes as well as chemical reactions must have reached some sort of dynamic equilibrium. So, boundary conditions of a periodicity type have been selected.

In our case, experimental results suggest that this periodicity regime has been obtained at the end of the wafer boat, i.e. on the 4th position of the test wafers. In the following, only this assumption has

been considered in the simulation runs. Perspectives for the case of a non periodical regime will be suggested later. In what follows, for concentrations, the profiles and their axial derivatives have been supposed to be identical for SiH_2, $SiHNH_2$ and SiH_3NH_2.

4. 2 First examples of simulation results

By lack of place, it must be pointed out that only a few significant results will be presented. In all the simulation runs, a temperature of 750°C, a pressure of 0.4 Torr and a silane/ammonia ratio equal to 0.4/.6 were adopted.

Radial concentration profiles for SiH_4, H_2, NH_3 and SiH_3NH_2 are displayed in Figure 5 to 8.

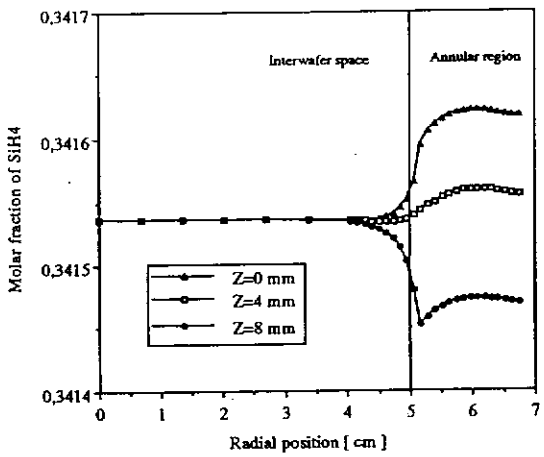

Figure 5 : Radial profile of silane molar fraction

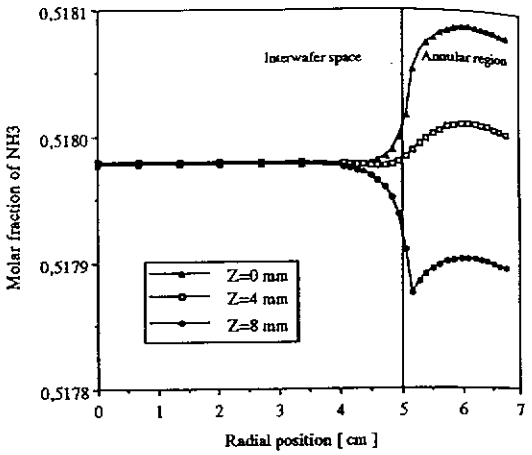

Figure 6 : Radial profile of ammonia molar fraction

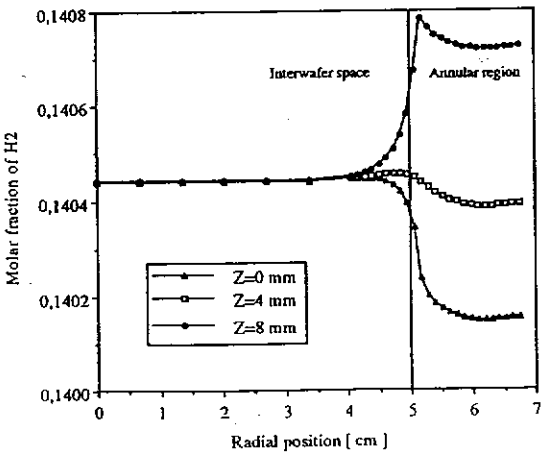

Figure 7: Radial profile of hydrogen molar fraction

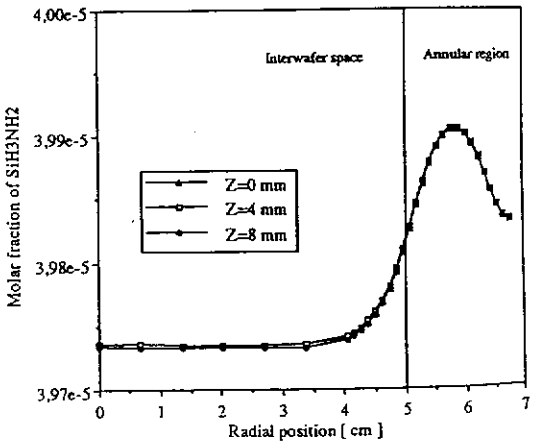

Figure 8 : Radial profile of SiH_3NH_2 molar fraction

They are relative to axial positions corresponding to the entrance, center and exit of the modelling field. As a first approximation, it can be concluded that all these species are uniformly distributed in the modelling field, in regard of the enlargement of the concentration scales. In more details, on the one hand, it can be said that silane and ammonia (respectively hydrogen) concentrations decrease

(respectively increases) from the entrance to the exit, due to the consumption (respectively production) of this species on solid surfaces by chemical reactions. In the case of SiH_3NH_2, no axial variations and only slight radial variations are observed. This species has a similar behavior to disilane in the case of polysilicon deposition [2] and may act as a storage for SiH_2 and $SiHNH_2$.

Figures 9 and 10 present radial concentration profiles for SiH_2 and $SiHNH_2$. It must be observed that their concentrations remain very low everywhere with a maximum value of 0.365 10^{-5} for SiH_2 (respectively of 0.405 10^{-5} for $SiHNH_2$). But their molar fraction varies widely in the modelling region and is function of the radial position (but not of the axial position) in the annular region. It is quite the opposite in the interwafer space, where the molar fraction is independent of the radial coordinate but varies with the axial position.

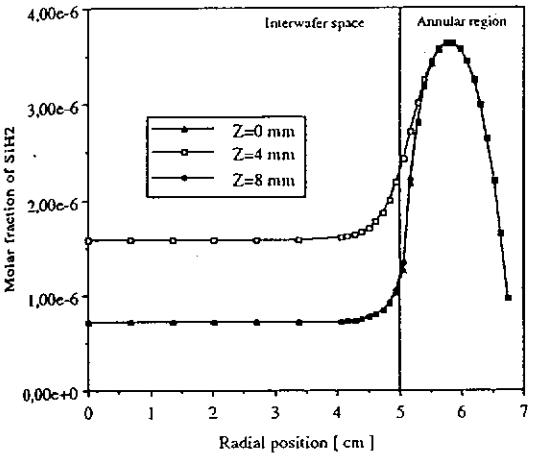

Figure 9 :Radial profile of SiH_2 molar fraction

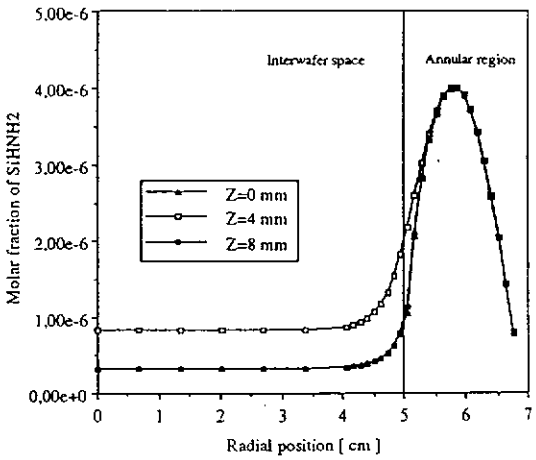

Figure 11 :Radial profile of $SiHNH_2$ molar fraction

Figure 11 represents silicon nitride deposition rate on the downstream side of the entrance wafer and indicates the contributions due to SiH_4, SiH_2, $SiHNH_2$, NH_3 at T = 750°C

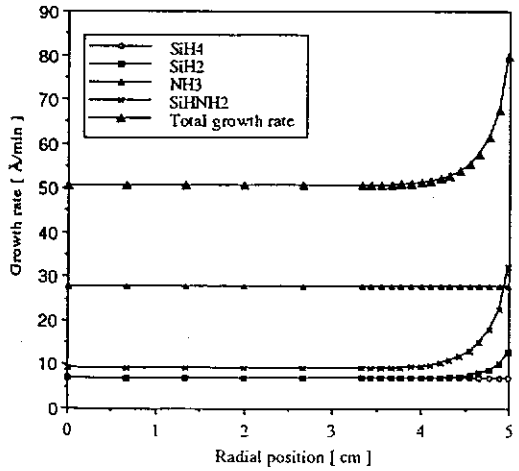

Figure 11 :Silicon nitride deposition rate

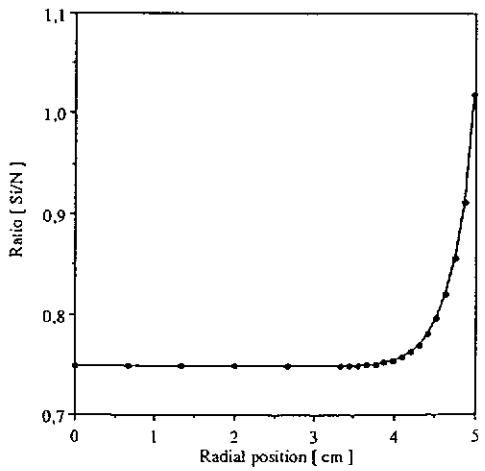

Figure 12 : Si/N ratio

Silane and ammonia contribution are uniform on the wafer. On the contrary, the SiH_2 and $SiHNH_2$ contributions are functions of position as a consequence of the important radial concentrations variations of these species. The same trend is observed at 650°C. Deposition rate has an order of magnitude of 10 Å/min in the center of the wafer and of 15 Å/min at the wafer edge. In view of the scarcity of kinetic information, the reasonable agreeement between model predictions and experiments is encouraging for the present modelling approach. Another result provided by the model concerns Si/N ratio (see Figure 12) deduced from the contributions of silicon and nitrogen to film elaboration. Simulation results show that silicon nitride films contain more silicon at the wafer edge, which may be related to the concentations of the reactive species in the vicinity of the wafer edge. These results have to be confirmed by measurements of Si/N ratio.

5- PERSPECTIVES AND CONCLUSIONS

The CVD2 model previously developed in our laboratory has been developed and applied to the specific example of silicon nitride deposition. Complex kinetic schemes involving both gas phase and surface reactions have been included in the model formulation. Considering the lack of detail information and kinetic parameters, the fit is encouraging for future investigations involving additional experimental data, concerning both film composition and deposition rate. Another perspective concerns the assumption of periodicity assumed in the model for SiH_3NH_2. Experiments have shown that on the first test wafer, positioned directly after a free volume without any wafer, deposition rate is higher than on the other wafers. This situation is similar to what happens after the entrance zone of a reactor, on the first wafers of the load. It can thus be suggested that SiH_3NH_2 acts as a storage tank for reactive species generated in the volume, i.e., SiH_2 and $SiHNH_2$. This assumption is now under investigation in our laboratory.

REFERENCES

[1]- Roenigk K.F., Jensen K.F., Low Pressure CVD of Silicon Nitride, J. Electrochem. Soc., 134, 1777-1785 (1987)

[2]- Duverneuil P., Couderc J.P., Two dimensional modelling of low pressure chemical vapor deposition hot wall tubular reactors (Part I), J. Electrochem. Soc., 139, 296-304 (1992)

[3]- Coltrin M. E., Kee R.J., Miller J.A., A mathematical model of silicon chemical vapor deposition - further refinements and the effects of thermal diffusion, J. Electrochem. Soc. , 133, 1207-1213 (1986)

[4]-Tachibana A., Yamaguchi K., Kawauchi S., Kurosaki Y., Yamabe T., SiH_3 Radical Mechanisms for Si-N Bond Formation, J. Am. Chem. Soc., 114, 7504-750 (1992)

[5]-Ishitani A., Koseki S., A model for SiN_x CVD film growth mechanism by using SiH_4 and NH_3 source gases, Japanese Journal of Applied Physics, 29, L2322-L2325 (1990)

[6]- Melius C.F., Ho P., Theoretical study of the thermochemistry of molecules in the Si-N-H-F system, J. Phys. Chem., 95, 1410-1419 (1991)

[7]- Benson S. W., Thermochemical kinetics, Wiley, Second Edition

[8]- Fayolle-Communal F., Analyse et modélisation des dépôts d'oxyde de silicium par procédé LPCVD, PhD Thesis, INPT (1993)

[9]- Azzaro C., Duverneuil P., Couderc J.P., Two dimensional modelling of low pressure chemical vapor deposition hot wall tubular reactors (Part II), J. Electrochem. Soc., 139, 305-312 (1992)

[10]- Wilke T.E., Turner K.A., Takoudis C.J., Chemical vapor deposition of silicon under reduced pressure in hot-wall reactors, Chem. Eng. Sci., 41, 643-650 (1986)

[11]- Azzaro C., Duverneuil P., Couderc J.P., Comments on the influence of the entrance zone in LPCVD reactors for in situ phosphorus doped polysilicon deposition, Chem. Engineering Journal, 48, 1915-1922 (1993)